Science
AAAS

Supplementary Materials for

Repair of CRISPR-guided RNA breaks enables site-specific RNA excision in human cells

Anna Nemudraia, Artem Nemudryi, Blake Wiedenheft

Corresponding authors: Artem Nemudryi, artem.nemudryi@gmail.com; Blake Wiedenheft, bwiedenheft@gmail.com

Science **384**, 808 (2024)
DOI: 10.1126/science.adk5518

The PDF file includes:

Other Supplementary Material for this manuscript includes the following:

Materials and Methods

Plasmids

pDAC627 (Addgene plasmid #195240; http://n2t.net/addgene:195240; RRID: Addgene_195240) and pDAC446 (Addgene plasmid # 195239; http://n2t.net/addgene:195239; RRID: Addgene_195239) expressing type III CRISPR-associated proteins from *Streptococcus thermophilus* (Csm2 – Csm5, Cas10, and Cas6) fused to a nuclear localization signal (NLS) and RNA guide, as well as pDAC569 (Addgene plasmid # 195241; http://n2t.net/addgene:195241; RRID:Addgene_195241) expressing nuclease-inactive SthCsm complex were gifts from Jennifer Doudna (*19*). To clone SthCsm guides targeting *PPIB*, *PARK7*, *XIST*, *CFTR*^{W1282X}, or reporter transcripts (stop-GFP, GFP-stop-Luc, fLuc-CFTR, and fLuc-CFTR^{W1282X}), pairs of complementary DNA oligos (table S1) were annealed and phosphorylated with T4 polynucleotide kinase [New England Biolabs (NEB)] as previously described (*3*). The resulting fragments were cloned using the *Bbs*I restriction enzyme (NEB) into pDAC627, pDAC446, or pDAC569. The unmodified vectors were used as the non-targeting control. Guide RNAs targeting *PPIB* and *PARK7* transcripts were designed using the *cas13design* algorithm (https://gitlab.com/sanjanalab/cas13), which was customized to select 32-nucleotide-long guide RNAs (*54*). Highest-ranking guide RNAs that target different regions of the transcripts were selected. The plasmids expressing crRNA alone or crRNA with Cas6-NLS protein were generated by ligation of PCR-amplified DNA from template plasmid pDAC627 (table S2).

To generate the plasmid expressing SthCsm complex without NLS tags (pAN052), the gene fragments were designed using the NEBuider online tool, synthesized (Twist Bioscience), and assembled using NEBuilder HiFi DNA Assembly Cloning Kit (NEB #E5520). Plasmid expressing crRNA within the 5`UTR of mCherry mRNA (pAN053) was generated using Q5 site-directed mutagenesis of pAN-CMV-mCherry-HA plasmid (SthCR_RFP_F and SthCR_RFP_R, table S3). The SthCsm guides were cloned as described above.

pSpCas9(BB)-2A-Puro (PX459) was a gift from Feng Zhang (Addgene plasmid #48139; http://n2t.net/addgene:48139; RRID:Addgene_48139). Cas9 sgRNAs targeting the *RTCB* gene were cloned as previously described (table S4) (*3*). Guide sequences were selected in the second and third exons of the gene using the inDelphi web interface based on predicted knockout efficiency and editing precision (https://indelphi.giffordlab.mit.edu/) (*60*).

pDF0159 pCMV - huDisCas7-11 mammalian expression plasmid was a gift from Omar Abudayyeh and Jonathan Gootenberg (Addgene plasmid #172507; http://n2t.net/addgene:172507; RRID:Addgene_172507) (*32*). To add the NLS tag to the N-terminus of the DisCas-11 protein and to introduce mutations (D1579R, Y311K, D987K) (*33*), the plasmid pDF0159 was modified using Q5 site-directed mutagenesis (table S3).

pDF0114 pu6-eco31i-eco31i-dis7-11-mature-dr-guide-scaffold was a gift from Omar Abudayyeh and Jonathan Gootenberg (Addgene plasmid #186981; http://n2t.net/addgene:186981 ; RRID: Addgene_186981) (*61*). To clone DisCas7-11 guides, two partially complementary DNA oligos were annealed and phosphorylated (table S5). The resulting duplexes were cloned into pDF0114 using *Bsa*I restriction enzyme (NEB) to substitute a non-targeting guide sequence.

To generate reporter plasmids pStop-GFP (pAN007) and pGFP-stop-Luc (pAN013), dscGFP-2A-Luciferase gene cassette was amplified from pGreenFire1-ISRE (EF1α-puro) vector (System Biosciences, TR016PA-P) using PCR and cloned in the pEGFP-N1 vector (Clontech) at the *Kpn*I and *Not*I restriction sites. Restriction sites and Flag-HA tag at the N-terminus of the GFP were

added into the overhangs of the oligonucleotide primers that were used for PCR. Stop codons were inserted in the 5'- or the 3'-end of the *gfp* gene using Q5 site-directed mutagenesis.

To generate the reporter plasmids fLuc-CFTR (pAN056) and fLuc-CFTR^{W1282X} (pAN057), the gene fragments were synthesized (Twist Bioscience) and assembled using NEBuilder HiFi DNA Assembly Cloning Kit (NEB #E5520). The firefly luciferase (fLuc) gene was fused with exons 22-27 of the *CFTR* gene, with or without the nonsense mutation. A synthetic intron (200 nt from 5'-end and 200 nt from 3'-end of the natural intron) was introduced between exons 24 and 25, such that the exon-exon junction in the spliced transcript is more than 50-55 nucleotides downstream of the stop codon, which is required for triggering the NMD (*35*).

Plasmid encoding for *RTCB* cDNA (pCMV-RTCB) was ordered from Genscript (Cat. No. OHu24215D).

All plasmid sequences were confirmed with whole-plasmid sequencing at Plasmidsaurus (https://www.plasmidsaurus.com/) (see plasmid sequences in Data S1 file).

Nucleic acids

All DNA oligos were purchased from Eurofins (table S1-S7).

Antibodies

Antibodies used for western blot: rabbit anti-RTCB (Proteintech, Cat:19809-1-AP, 1:1000), rabbit anti-ACTB (ABclonal, Cat: AC026, 1:20,000), goat anti-rabbit IgG peroxidase-conjugated (Jackson ImmunoResearch, Cat: 111-035-003, 1:10,000), goat anti-mouse AlexaFluor488 (Invitrogen, A11001, 1:2000), goat anti-rabbit AlexaFluor 594 (Invitrogen, A11012). The CFTR antibodies mouse anti-NBD2 (596; dilution 1:2500) were purchased through the Cystic Fibrosis Foundation Therapeutics Antibody Distribution Program (CFF, Bethesda, MD, USA). Antibodies used for immunocytochemistry: anti-FLAG (Sigma, F1804, 1:2000), goat anti-mouse AlexaFluor488 (Invitrogen, A11001, 1:2000).

Immunocytochemistry

293T cells were transfected with plasmid DNA using FuGENE HD reagent (Promega) according to the manufacturer's instructions. 24 hours after transfection, cells were detached and seeded at 50% confluency on glass coverslips (Fisherbrand, #12-545-80) pre-coated with poly-D-lysine (Cultrex, #3439-100-01) in a 24-well plate. The next day, media was removed, cells were washed with PBS and fixed with 4% paraformaldehyde for 10 min. The cells were washed three times with PBS and permeabilized with 0.5% TritonX-100 in PBS for 10 min at RT. Cells were blocked with 1% BSA in PBS with 0.05% Tween-20 for 1 hour at RT. After blocking, the cells were stained overnight at 4°C with anti-FLAG antibodies diluted in a blocking buffer. The next day, cells were washed three times in PBS and stained with secondary antibodies diluted in a blocking buffer for 1 hour at RT in the dark (goat anti-mouse AlexaFluor488; Invitrogen, A11001). After 3x PBS washes, nuclei were stained with Hoechst 33342 in PBS for 5 minutes at RT. Coverslips were then mounted with ProLong Gold antifade mounting media (Invitrogen, P36934) on Superfrost Plus microscope slides (#22-037-246). Immunostained cells were imaged using Nikon Ti-Eclipse inverted microscope (Nikon Instruments) equipped with a SpectraX LED excitation module (Lumencor) and emission filter wheels (Prior Scientific). Fluorescence imaging used excitation/emission filters and dichroic mirrors for GFP and DAPI (Chroma

Technology Corp.). Images were acquired with Plan Fluor 20Ph objective and an iXon 896 EM-CCD camera (Andor Technology Ltd.) in NIS-Elements software.

Cell cultures

293T cells (ATCC, CRL-3216) were maintained at 37ºC and 5% CO2 in Dulbecco's Modified Eagle Medium (DMEM, GIBCO, cat. #12100-061) supplemented with 10% fetal bovine serum (FBS, ATLAS Biologicals, Lot. #F31E18D1), sodium bicarbonate (3.7 g/L), 50 I.U./mL penicillin and 50 mg/mL streptomycin. CFF-16HBEge CFTR W1282X cells (Cystic Fibrosis Foundation, Bethesda, MD, USA) were maintained at 37ºC and 5% CO2 in Modified Eagle Medium (MEM, GIBCO, cat. #12100-061) supplemented with 10% fetal bovine serum (FBS, ATLAS Biologicals), 50 I.U./mL penicillin and 50 mg/mL streptomycin. The cells tested PCR-negative for mycoplasma.

RTCB depletion

To deplete RTCB, 293T cells were transfected using Lipofectamine 3000 (ThermoFisher Scientific) with the plasmid encoding for Cas9, puromycin resistance protein, and a guide RNA targeting the *RTCB* gene. Twenty-four hours post-transfection, the media was changed to the media with puromycin (1 µg/mL), and the cells were selected for three days. After selection, cells were seeded on 96-well plates at 3 cells per well density to generate clonal cell lines. Cell clones were monitored for 14 days, and wells with single colonies were marked and used to determine knockout efficiencies. To determine knock-out efficiency, the genomic DNA from bulk populations or clonal cell lines was extracted using DNeasy Blood & Tissue Kit (QIAGEN), and targeted genome regions were amplified with Q5 polymerase (NEB) (table S6). Amplicons were Sanger-sequenced (Psomagen), and resulting traces (i.e., ab1 files) were used to quantify indels with the ICE software from Synthego (https://ice.synthego.com) (*62*).

Plasmid transfection

293T cells were seeded one or two days before the experiment and transfected when ~80-90% confluency was reached. For the experiment shown in Fig. 1B and Fig. 2C, 500 ng of plasmid DNA encoding for SthCsm complex and guide RNA was mixed with 1.5 µL of FuGENE HD reagent (Promega), incubated for 15 min, and added to the well of a 24-well plate. Twelve hours post-transfection, the cells were detached and seeded on 12-well plates in a media with puromycin (1 µg/mL). Three days after puromycin selection, the total RNA was extracted from cells using RNeasy Plus Mini Kit (QIAGEN, # 74134). For the experiment shown in Fig. 1E-H, transfection was performed as described above but without puromycin selection.

For the experiment shown in Fig. 4, the cells were seeded in a 96-well plate in ~80-90% confluency. For editing with SthCsm complex, 100 ng of plasmid encoding for SthCsm and 50 ng of plasmid encoding for a reporter (stop-GFP or GFP-stop-Luc) were mixed with 0.8 µL FuGENE HD reagent (Promega), incubated for 10 min, and added to the well. For editing with DisCas7-11, 100 ng of plasmid encoding for DisCas7-11, 50 ng of the plasmid encoding for guide RNA, and 50 ng of the plasmid encoding for the GFP-stop-Luc reporter were mixed with 1.1 µ FuGENE HD reagent (Promega), incubated for 10 min, and added to the wells. Forty-eight hours post-transfection, the cells were imaged with the Nikon Ti-Eclipse inverted microscope (Nikon Instruments) equipped with a SpectraX LED excitation module (Lumencor) and emission filter wheels (Prior Scientific) (for the reporter stop-GFP). Fluorescence imaging used excitation/emission filters and dichroic mirrors for GFP (Chroma Technology Corp). Images

were acquired with Plan Fluor 20Ph objective and an iXon 896 EM-CCD camera (Andor Technology Ltd.) in NIS-Elements software. For luciferase assays, media was removed, and cells were lysed in 50 µL of the 1X Cell Culture Lysis Reagent (Promega). Lysates were used for luciferase assays (20 µL) with Luciferase assay system (Promega) and RNA extraction (20 µL) with RNeasy Plus Mini Kit (QIAGEN, # 74134).

For the experiment shown in Fig. 5, the CFF-16HBEge cells were transfected using the reverse-transfection method. First, 2 µg of the plasmid DNA was mixed with 6 µL FuGENE HD reagent (Promega), incubated for 10 min, and added to the well of a 12-well plate. Then, 160,000 cells were added per well. Twelve hours post-transfection, the media was changed for the media with puromycin (0.75 µg/mL). Two days after puromycin selection, the total RNA was extracted from cells using the RNeasy Plus Mini Kit (QIAGEN, # 74134).

RT-qPCR

Total RNA from cells was extracted with RNeasy Plus Mini Kit (QIAGEN, # 74134). The reverse-transcription (RT) reactions were performed with 2X LunaScript RT SuperMix Kit (NEB) with 5 µL of RNA input (250 ng of RNA total) in 10 µL total reaction volume. The RT reactions containing cDNA were diluted 100-fold, and 5 µL was used for qPCR reactions with 2X Universal SYBR Green Fast qPCR Mix (ABClonal). Each qPCR reaction contained 5 µL of cDNA, 4.2 µL of Nuclease-free Water, 0.4 µL of 10 mM Primers (table S7), and 10 µL of 2X mastermix. Nuclease-free water was used as no template control (NTC). Three technical replicates were performed for each sample. Amplification was performed in QuantStudio 3 Real-Time PCR System instrument (Applied Biosystems) as follows: 95°C for 3 min, 40 cycles of 95°C for 5 s, and 60°C for 30 s, followed by Melt Curve analysis. Results were analyzed in Design and Analysis application at Thermo Fisher Connect Platform.

Nanopore sequencing

Amplicons from RT-qPCR reactions were purified with magnetic beads (Mag-Bind® TotalPure NGS), and ~13 ng of DNA was used to prepare sequencing libraries as described in SQK-LSK114 protocol using Native Barcoding Kit 24 V14 (SQK-NBD114.24) or Native Barcoding Kit 96 V14 (SQK-NBD114.96). Edited *XIST* RNA was reverse-transcribed using the LunaScript RT SuperMix Kit (NEB), and cDNA was used for PCR with primers XIST_seq_F and XIST_seq_R (table S7) and Q5 polymerase (NEB). Amplicons were purified with magnetic beads (Mag-Bind® TotalPure NGS), and ~13 ng of DNA was used to prepare sequencing libraries as described in SQK-LSK114 protocol using Native Barcoding Kit 24 V14 (SQK-NBD114.24). ~20 fM of the library was loaded on the Nanopore MinION [R10.4.1 flow cell, accurate mode (260 bases per second)]. The flow cell was primed, and sequencing libraries were loaded according to the Oxford Nanopore protocol (SQK-LSK114). The sequencing run was performed in the fast base calling mode in the MinKNOW software. After the run, raw sequencing data (POD5 files) was re-basecalled with the super-accuracy model (dna_r10.4.1_e8.2_260bps_sup@v4.1.0) using and demultiplexed with Dorado basecaller (v0.3.3, Oxford Nanopore).

Sequencing data analysis

Sequencing reads were aligned to the reference using *minimap2* (v2.17 -r954-dirty) with Nanopore preset (-ax map-ont setting). Alignments were converted to BAM format, sorted, and indexed using *samtools* v1.13. Sequencing reads were trimmed to remove primer binding regions

using the *samtools ampliconclip*. To make sequencing depth plots, a subset of reads was randomly selected using *samtools view*. Sequencing depth was computed with the *samtools depth*. Deletions in sequencing reads were quantified using the extract-junctions.py script (github.com/hyeshik/sars-cov-2-transcriptome/blob/master/nanopore/_scripts/extract-junctions.py) (*63*). Deletion counts at the SthCsm target sites were normalized to the number of reads that span the target region, which was computed by extracting read information from BAM files using the *bamtobed* function in *bedtools* v2.30.0 package and filtering reads by start and end coordinate (Data S1). All plots were created using *ggplot2* v3.3.5 package in RStudio software v2023.03.0.

Western blot

Cells were washed two times with PBS and lysed in RIPA buffer (150 mM sodium chloride, 1% NP-40, 0.5% sodium deoxycholate, 0.2% SDS, 50 mM Tris, pH 8.0) at 4ºC for 30 min. The lysates were clarified by centrifugation (20 min at 10,000 g) and stored at -80ºC. Lysates were mixed with 6X Laemmli buffer, heated at 98ºC for 5 min, resolved in 12% SDS-PAGE gel, and transferred onto a nitrocellulose membrane using Mini Trans-Blot Electrophoretic Transfer Cell (Bio-Rad, #1703930). Membranes were stained with Ponceau S, imaged, washed, blocked, and probed with indicated antibodies. The proteins were visualized using Pierce ECL Western Blotting Substrate (ThermoFisher Scientific, #32106) and exposed to X-Ray film (sc-201696, Santa Cruz Biotech).

Statistical analysis

All experiments were performed in biological triplicates. All RT-qPCR reactions were performed in three biological replicates, each with three technical replicates. Pairwise comparisons were performed in R with Welch's unequal variances *t*-test using the *t.test* function from the *stats* package. One-way ANOVA was performed using the *aov* function from the *stats* package in R. Post-hoc multiple pairwise comparisons were performed with Dunnett's test using the *glht* function from the *multcomp* R package (Fig. 4E) and Tukey's test using the *TukeyHSD* function from the *stats* R package (Fig. 2F). Significance levels: $*P < 0.05$, $**P < 0.01$, $***P < 0.001$.

Supplementary Text

RTCB knockout

There are three copies of the *RTCB* gene in 293T cells, and after testing 41 clones, we have not identified any with a complete knockout (*64*) (**fig. S3D**). These results are consistent with work showing that *RTCB* is essential (*24-26*). However, we have identified clones with a knockout of two copies of the gene, which results in a substantial depletion of the RTCB protein (**Fig. 2B; fig. S3**).

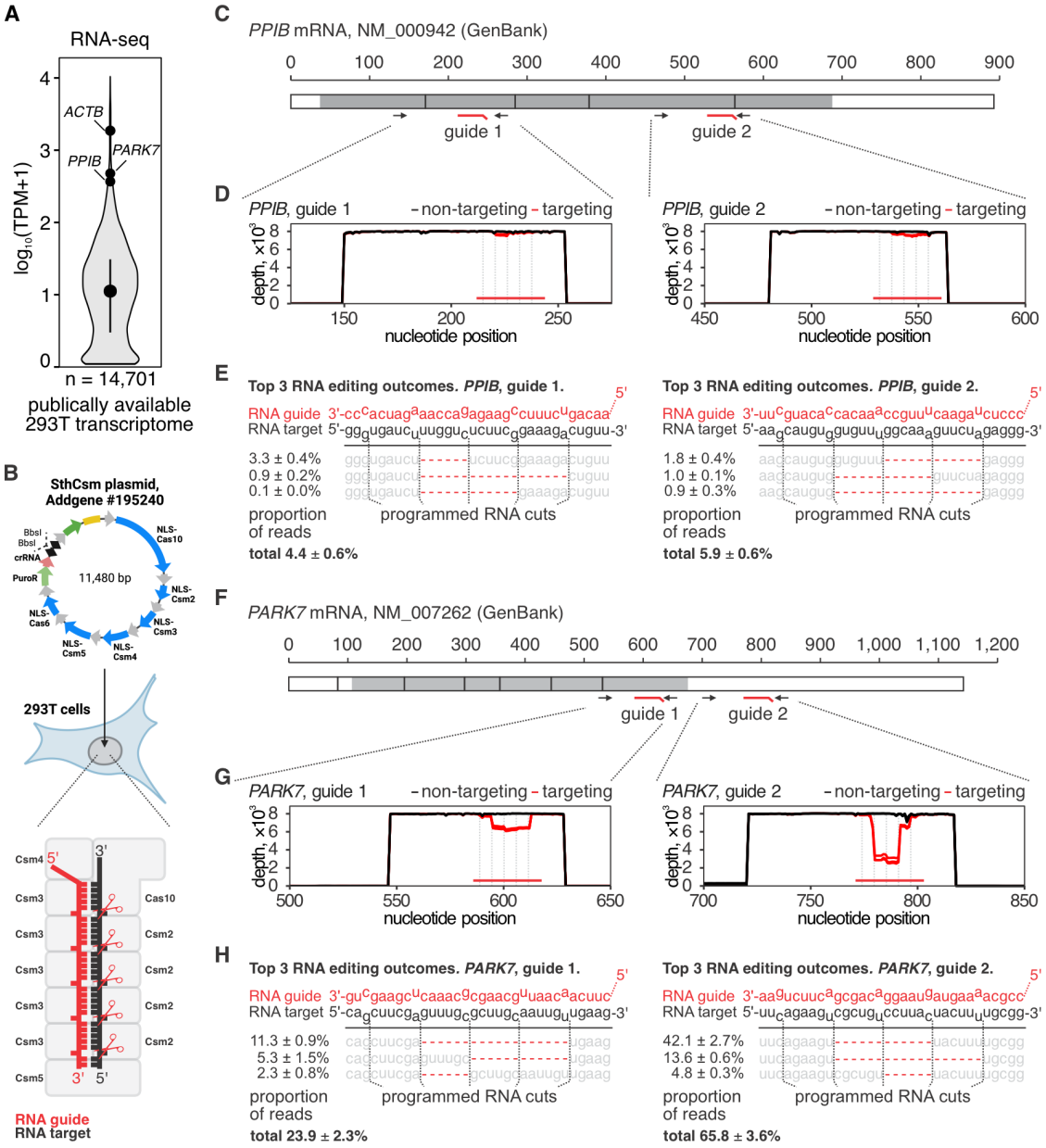

Fig. S1. The distribution and frequency of RNA editing outcomes in *PPIB* and *PARK7* mRNAs. A) Publicly available gene expression data from Human Protein Atlas (https://www.proteinatlas.org/about/download) was used to generate a violin plot. The y-axis shows expression of human genes in 293T cells (n = 14,701 genes with non-zero expression). TPM – transcripts per million. The vertical black line shows the interquartile range. The black dot shows the median expression level. **B)** *Top:* Diagram of the plasmid (Addgene #195240) encoding for human codon-optimized and NLS-tagged protein subunits of the type III-A CRISPR-Csm complex from *Streptococcus thermophilus* (SthCsm), CRISPR RNA (crRNA) - processing nuclease Cas6, and single-spacer CRISPR array. CRISPR repeats are shown as black diamonds. The sequence between the repeats has two BbsI restriction sites for cloning spacers for targeting complementary target RNAs. *Bottom:* Diagram of the assembled SthCsm ribonucleoprotein complex bound to the target RNA (black). crRNA is shown with red color.

The target RNA is cleaved in six nucleotide intervals by Csm3 nucleases in the backbone of the complex. Cleavage sites are indicated with red scissors. **C)** Diagram of the *PPIB* mRNA (NM_000942, GenBank). The scale shows nucleotide position along the transcript. Blocks show exons in the spliced mRNA, gray color indicates the position of the PPIB open reading frame (ORF). Red lines mark the position of the SthCsm guide RNAs. Black arrows indicate the position of the binding sites for oligonucleotide primers used for RT-qPCR in Fig. 1B. **D)** qPCR amplicons were deep-sequenced, and resulting reads were aligned to the reference sequences. A subset of 8,000 reads was randomly selected from the alignment for the representation. Plots show sequencing coverage (y-axes) along the length of the amplicons (x-axes). Each line represents a single replicate, three replicates total per guide RNA. Vertical dotted gray lines indicate predicted RNA break sites. The horizontal red line shows the position of the guide RNA with respect to the target. **E)** Top three most frequent RNA editing outcomes in PPIB transcript. Dotted lines indicate the positions of RNA breaks introduced with the CRISPR complex. Red dashes depict deletions identified in the sequencing data. Deletion frequency was quantified as the mean ± one standard deviation of three biological replicates. **F)** Same as in **(C)** but for the *PARK7* transcript (NM_007262, GenBank). **G)** Same as in (**D**) but for target sites in the *PARK7* transcript. **H)** Top three most frequent RNA editing outcomes at the target sites in *PARK7*. Data is shown as the mean ± one standard deviation of three biological replicates.

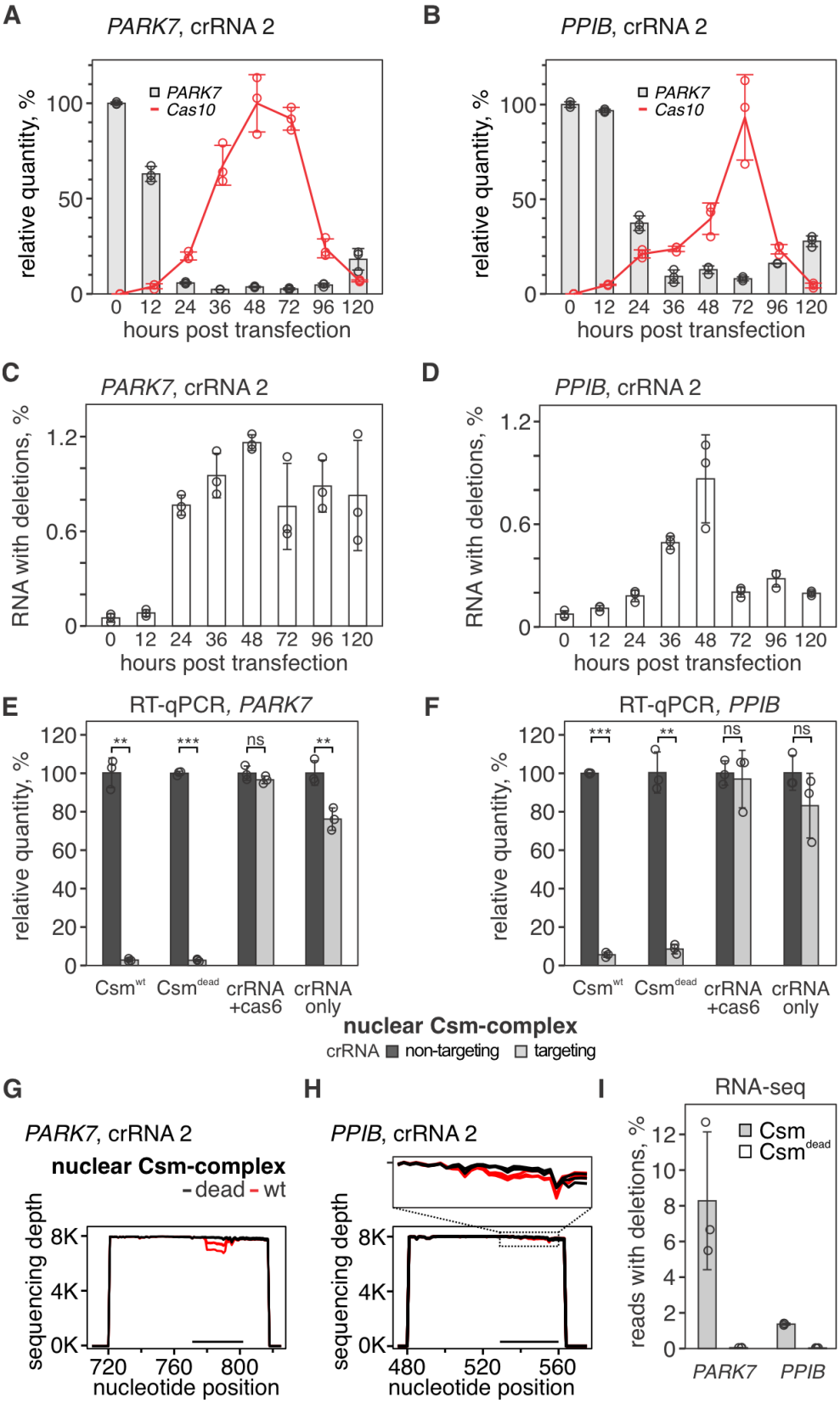

Fig. S2. Kinetics of RNA repair and cytoplasmic RNA knockdown with active and inactive Csm-complexes. A) Kinetics of *PARK7* mRNA knockdown (guide 2) vs. expression of the

cas10 gene from the NLS-tagged SthCsm complex expression. The same data as in main Fig. 1E. Data was included here for comparison with *PPIB* data. **B)** Same as in **(A)** but for the *PPIB* transcript (guide 2). **C)** *PARK7* qPCR products in **(A)** were sequenced, and deletion efficiency was calculated as [relative quantity] × [fraction of reads with deletions]. The same data as in main Fig. 1F. Data was included here for comparison with *PPIB* data. **D)** Same as in **(C)** but for the *PPIB* transcript. **E)** *PARK7* knockdown efficiencies with "wildtype" NLS-tagged SthCsm complex (Csm^{wt}), catalytically inactive NLS-tagged SthCsm complex (Csm^{dead}), crRNA expressed only with Cas6 gene (no Csm genes), and cRNA alone were measured using RT-qPCR. Welch's t-test was used to compare samples expressing targeting and non-targeting crRNA. ** - $p < 0.01$, *** - $p < 0.001$, ns – non-significant. The same data as in main Fig. 1G. Data was included here for comparison with *PPIB* data. **F)** Same as in **(E)** but for *PPIB*. **G)** RT-qPCR amplicons in **(E)** were sequenced, and reads were aligned to reference as in fig. S1G. A subset of 8,000 reads was randomly selected from the alignment for the representation. The plot shows sequencing depth (y-axis) along the length of the amplicon (x-axis). Each line represents a single replicate, with three replicates total per Csm-complex. Horizontal black bar shows position of the sequence targeted with the Csm-complex. **H)** Same as in **(G)** but for *PPIB*. The inset on top shows the zoom-in on the region targeted with Csm-complex (dotted box). **I)** Quantification of data in **(G)** and **(H)**.
.

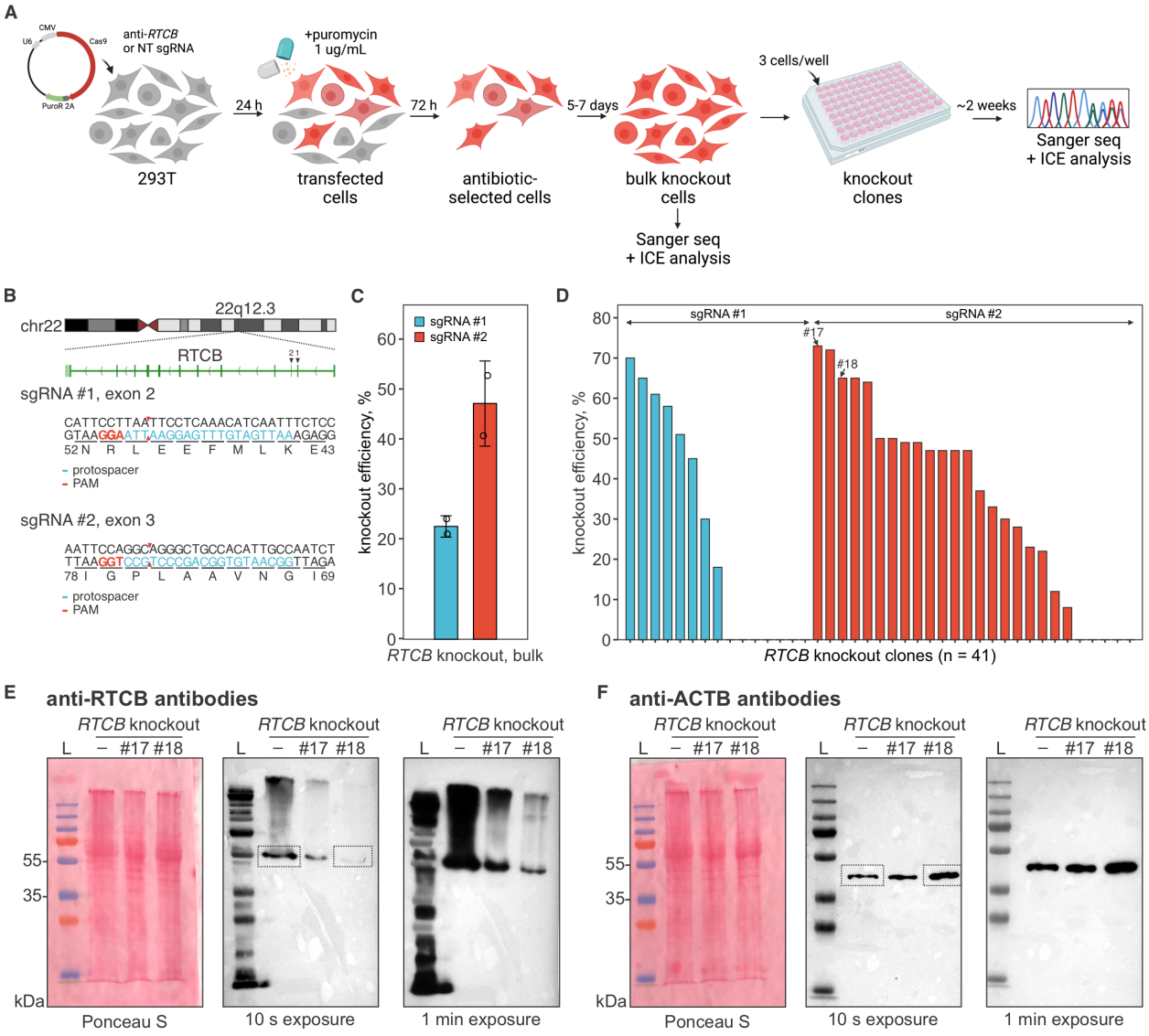

Fig. S3. Knockout of RTCB gene with CRISPR-Cas9. A) Schematics of the knockout strategy. **B)** Diagram showing the exon-intron structure of the *RTCB* gene (top), and sequences targeted with Cas9 (middle and bottom). **C)** *RTCB* knockout efficiency in bulk cells was quantified by analyzing Sanger traces from target site amplicons using the ICE web tool (Synthego). **D)** Quantification of *RTCB* knockout efficiency in 293T cell clones. **E and F)** Clones #17 and #18, indicated with black arrows in (**D**), were lysed, and lysates were probed with anti-RTCB or anti-ACTB antibodies. Dotted boxes show parts of the images that were cropped out for main Fig. 2B.

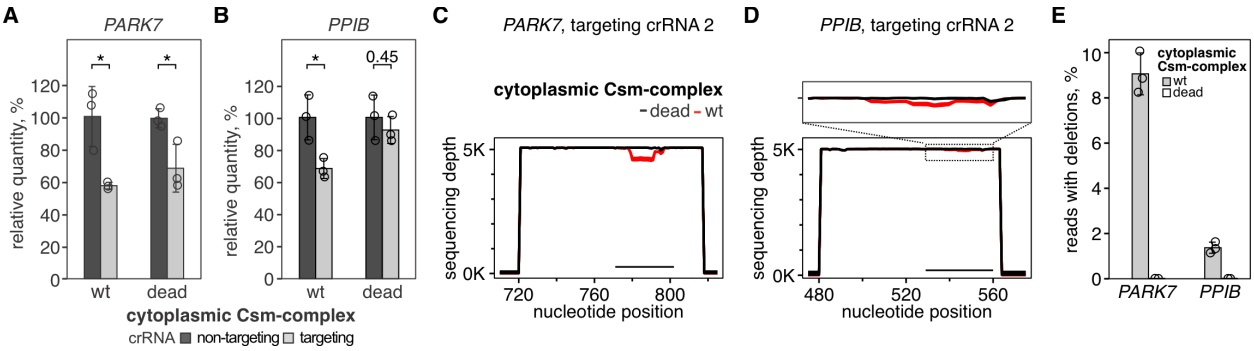

Fig. S4. Targeting nuclear-exported transcripts *PARK7* and *PPIB* with cytoplasmic SthCsm-complex. A, B) Knockdown of *PARK7* (A) and *PPIB* (B) transcripts with cytoplasmic SthCsm (no NLS). Data in (A) is the same as in main Fig. 2H and was included for comparison with *PPIB* targeting. Transcript levels were quantified with RT-qPCR and normalized to *ACTB* and non-targeting control. "wt" – nuclease-active SthCsm, "dead"– catalytically inactivated SthCsm (Csm3^{D33A} mutation). *p-value < 0.05, ns – non-significant; Welch's t-test. Data is shown as mean (n = 3) ± one standard deviation. **C, D)** RT-qPCR amplicons in (A) and (B) were deep-sequenced, and reads were aligned to reference sequences. Analysis was performed as in fig. S1 and fig. S2. **E)** Quantification of data in (C) and (D).

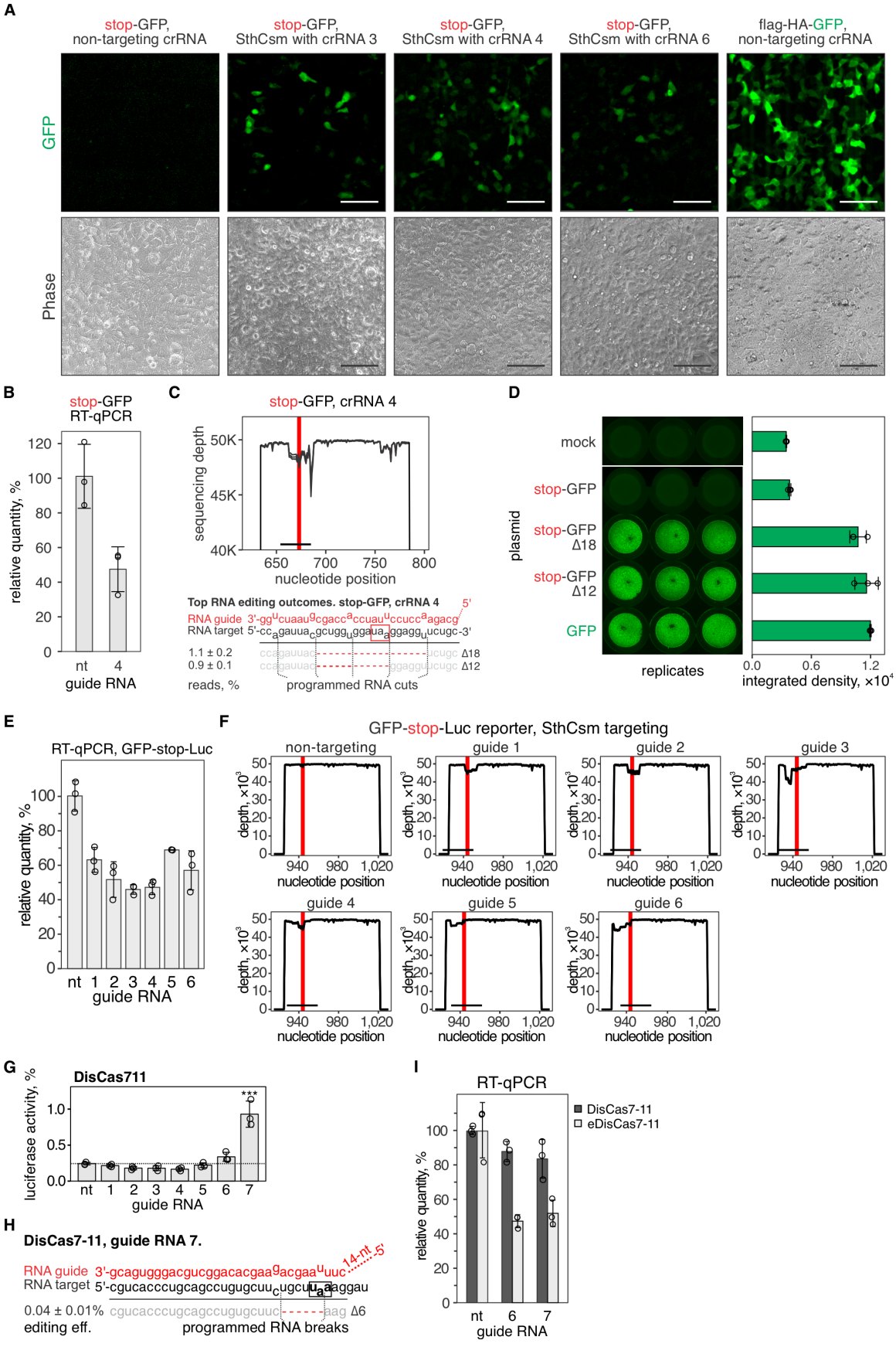
A
stop-GFP, non-targeting crRNA
stop-GFP, SthCsm with crRNA 3
stop-GFP, SthCsm with crRNA 4
stop-GFP, SthCsm with crRNA 6
flag-HA-GFP, non-targeting crRNA
GFP
Phase
B
stop-GFP RT-qPCR
relative quantity, %
guide RNA
C
stop-GFP, crRNA 4
sequencing depth
nucleotide position
Top RNA editing outcomes. stop-GFP, crRNA 4
RNA guide
RNA target
reads, %
programmed RNA cuts
D
mock
stop-GFP
stop-GFP Δ18
stop-GFP Δ12
GFP
plasmid
replicates
integrated density, ×10^4
E
RT-qPCR, GFP-stop-Luc
relative quantity, %
guide RNA
F
GFP-stop-Luc reporter, SthCsm targeting
non-targeting
guide 1
guide 2
guide 3
guide 4
guide 5
guide 6
depth, ×10^3
nucleotide position
G
DisCas711
luciferase activity, %
guide RNA
H
DisCas7-11, guide RNA 7.
RNA guide
RNA target
editing eff.
programmed RNA breaks
I
RT-qPCR
DisCas7-11
eDisCas7-11
relative quantity, %
guide RNA

Fig. S5. Programmable deletion of stop codons in RNA restores protein expression.
A) Fluorescent imaging of cells transfected with plasmids for the stop-GFP reporter and SthCsm with a non-targeting guide (left), stop-GFP reporter and SthCsm with targeting guides, or GFP reporter and SthCsm with the non-targeting guide (right). Scale bars – 50 μm. **B)** RT-qPCR was used to quantify stop-GFP reporter RNA in cells transfected with plasmids encoding for SthCsm complex and non-targeting crRNA (NT) or targeting crRNA 4. **C)** *Top:* RT-qPCR products were sequenced, and sequencing depth (*y-axis*) was calculated and plotted against the position in the reporter RNA (*x-axis*) (*top*). The horizontal black bar marks the target sequence in the reporter. The vertical red line highlights the stop codon. *Bottom:* two most frequent deletions in the target RNA. The red box marks the stop codon (UAA). **D)** Site-directed mutagenesis was used to make deletions identified in **(C)** into the stop-GFP reporter plasmid. Mutagenized plasmids were used to transfect 293T cells, and cell culture plates were imaged 48 hours post-transfection using the Typhoon scanner (*left*). The fluorescent signal (integrated density) was quantified in ImageJ and plotted as a bar graph (*right*). **E)** RNA was extracted from the same lysates that were used in luciferase assays shown in Fig. 4E. RT-qPCR was performed with oligonucleotide primers that flank the region targeted with SthCsm in the GFP-stop-Luc reporter transcript. Transcript quantities are normalized to *ACTB* and non-targeting guide RNA control using the ΔΔCt method. The mean ± one standard deviation of three biological replicates is shown. nt – non-targeting guide RNA. **F)** Deep sequencing of qPCR amplicons in (**E**). Reads were aligned to the reference sequence of the GFP-stop-Luc reporter. Graphs show sequencing depth (*y-axes*) at the amplified region of the transcript (*x-axes*). Every line shows a biological replicate (n = 3). The horizontal black bar indicates a region complementary to the guide RNA of the SthCsm complex. Vertical red lines mark the position of the stop codon targeted with SthCsm. **G)** Luciferase activity was measured in cell lysates 48 hours after transfection with GFP-stop-Luc and DisCas7-11 plasmids. Luciferase activity is normalized to a control transfected with a reporter plasmid without the stop codon. Data are shown as mean ± one standard deviation of three replicates. Means were compared using one-way ANOVA, and samples with targeting guide RNAs were compared to the non-targeting control using one-tailed Dunnett's test. *** $p < 0.001$. **H)** Frequency of RNA editing with DisCas7-11 and guide 7. Editing efficiency was quantified as mean ± one standard deviation of three biological replicates. The black box shows the stop codon that was targeted by DisCas7-11. **I)** RNA was extracted from the same lysates that were used in luciferase assays shown in **(G)**(DisCas7-11) and main Fig. 4H (eDisCas7-11). RT-qPCR was performed with oligonucleotide primers that flank the target region in the GFP-stop-Luc reporter transcript. Transcript quantities are normalized to *ACTB* and non-targeting guide RNA control using the ΔΔCt method. The mean ± one standard deviation of three biological replicates is shown. nt – non-targeting guide RNA.

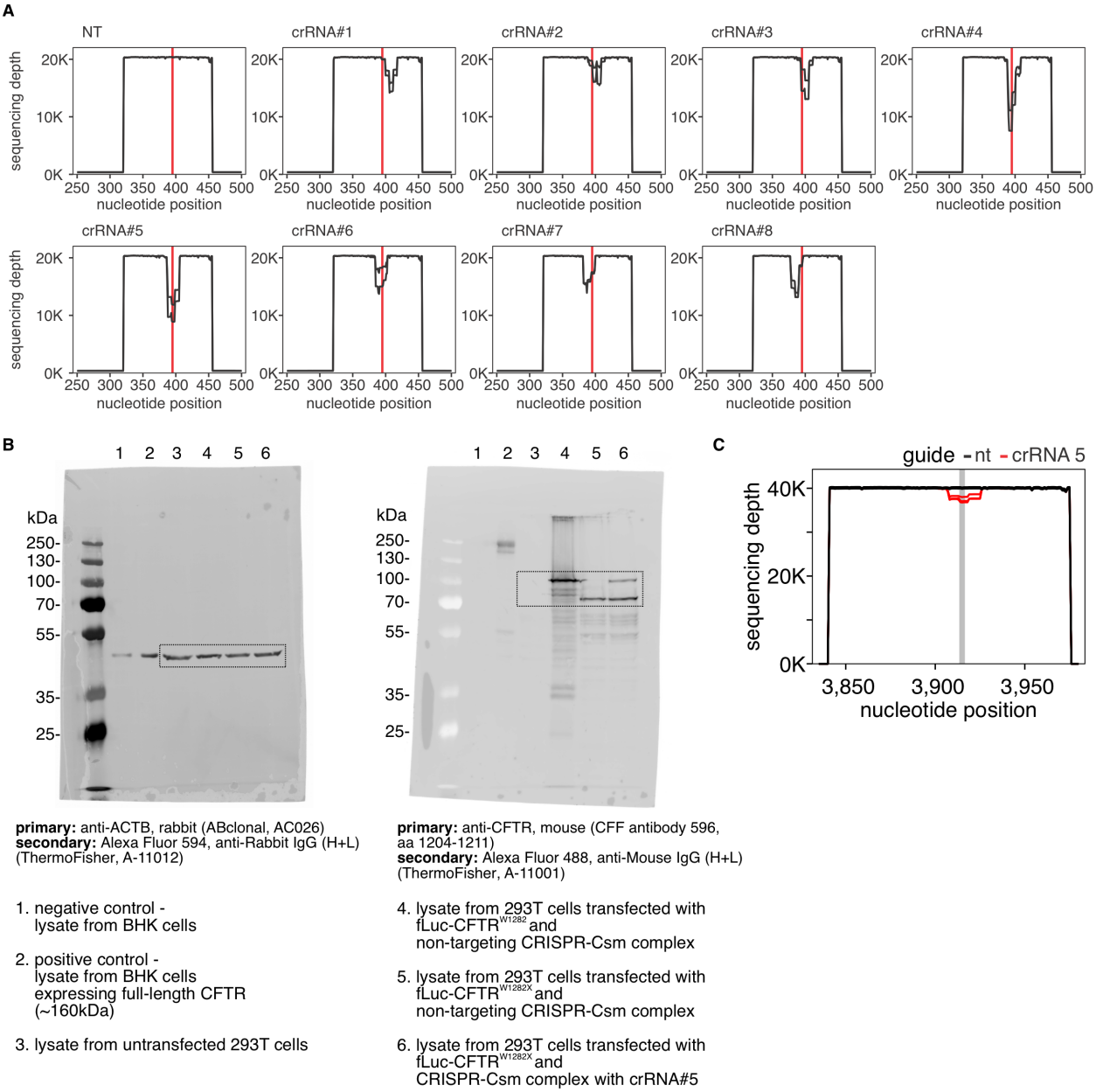

Fig. S6. Programmable excision of W1282X premature stop codon in *CFTR* transcript. A) Deep-sequencing of qPCR amplicons in Fig. 5B. Reads were aligned to the reference sequence of the fLuc-CFTR reporter. Graphs show sequencing depth (y-axes) at the amplified region of the transcript (x-axes). Every line shows a biological replicate (n = 2). Vertical red lines mark the position of the stop codon targeted with SthCsm. **B)** Uncropped western blot images for Fig. 5D. Dotted boxes show parts of the images that were cropped out. **C)** Deep-sequencing of qPCR amplicons in Fig. 5F. Reads were aligned to the reference sequence of the *CFTR* (NM_000492.4, GenBank). Graph show sequencing depth (*y-axis*) at the amplified region of the transcript (*x-axis*). Every line shows a biological replicate (n = 3).

Table S1.

Oligonucleotides used for cloning SthCsm guide RNAs

Name	Sequence 5`-3`
Guides targeting endogenous transcripts	
PPIB_g1F	AAACAACAGTCTTTCCGAAGAGACCAAAGATCACCC
PPIB_g1R	TATCGGGTGATCTTTGGTCTCTTCGGAAAGACTGTT
PPIB_g2F	AAACCCCTCTAGAACTTTGCCAAACACCACATGCTT
PPIB_g2R	TATCAAGCATGTGGTGTTTGGCAAAGTTCTAGAGGG
PARK7_g1F	AAACCTTCAACAATTGCAAGCGCAAACTCGAAGCTG
PARK7_g1R	TATCCAGCTTCGAGTTTGCGCTTGCAATTGTTGAAG
PARK7_g2F	AAACCCGCAAAAGTAGTAAGGACAGCGACTTCTGAA
PARK7_g2R	TATCTTCAGAAGTCGCTGTCCTTACTACTTTTGCGG
XIST_cr1F	AAACTAAAACCAGGTATCCGCAGCCCCGATGGGCAA
XIST_cr1R	TATCTTGCCCATCGGGGCTGCGGATACCTGGTTTTA
XIST_cr2F	AAACAAAAGCAGATATCCGTCACCCCGATGGGCCAG
XIST_cr2R	TATCCTGGCCCATCGGGGTGACGGATATCTGCTTTT
XIST_cr3F	AAACAAAAAGCAGGTATCCGAAGCCCCGATGGGCCA
XIST_cr3R	TATCTGGCCCATCGGGGCTTCGGATACCTGCTTTTT
XIST_cr4F	AAACAAAATCAAAGCAGGTATCCGCGGCCCCGATGG
XIST_cr4R	TATCCCATCGGGGCCGCGGATACCTGCTTTGATTTT
Guides targeting stop-GFP reporter	
sthcsm_stop_gfp_g1F	AAACGCGGCGGGGGCAGAACCTCCTTATCCACCAGC
sthcsm_stop_gfp_g1R	TATCGCTGGTGGATAAGGAGGTTCTGCCCCCGCCGC
sthcsm_stop_gfp_g2F	AAACGCGGGGGCAGAACCTCCTTATCCACCAGCGTA
sthcsm_stop_gfp_g2R	TATCTACGCTGGTGGATAAGGAGGTTCTGCCCCCGC
sthcsm_stop_gfp_g3F	AAACGGGGCAGAACCTCCTTATCCACCAGCGTAATC
sthcsm_stop_gfp_g3R	TATCGATTACGCTGGTGGATAAGGAGGTTCTGCCCC
sthcsm_stop_gfp_g4F	AAACGCAGAACCTCCTTATCCACCAGCGTAATCTGG
sthcsm_stop_gfp_g4R	TATCCCAGATTACGCTGGTGGATAAGGAGGTTCTGC
sthcsm_stop_gfp_g5F	AAACGAACCTCCTTATCCACCAGCGTAATCTGGAAC
sthcsm_stop_gfp_g5R	TATCGTTCCAGATTACGCTGGTGGATAAGGAGGTTC
sthcsm_stop_gfp_g6F	AAACCCTCCTTATCCACCAGCGTAATCTGGAACATC
sthcsm_stop_gfp_g6R	TATCGATGTTCCAGATTACGCTGGTGGATAAGGAGG
Guides targeting GFP-stop-Luc reporter	
csm_gfp_stop_luc_g1F	AAACTCACCGGTCACATTGATCCTTTAAGCAGAAGC
csm_gfp_stop_luc_g1R	TATCGCTTCTGCTTAAAGGATCAATGTGACCGGTGA
csm_gfp_stop_luc_g2F	AAACCCGGTCACATTGATCCTTTAAGCAGAAGCACA
csm_gfp_stop_luc_g2R	TATCTGTGCTTCTGCTTAAAGGATCAATGTGACCGG
csm_gfp_stop_luc_g3F	AAACGTCACATTGATCCTTTAAGCAGAAGCACAGGC

csm_gfp_stop_luc_g3R	TATCGCCTGTGCTTCTGCTTAAAGGATCAATGTGAC
csm_gfp_stop_luc_g4F	AAACACATTGATCCTTTAAGCAGAAGCACAGGCTGC
csm_gfp_stop_luc_g4R	TATCGCAGCCTGTGCTTCTGCTTAAAGGATCAATGT
csm_gfp_stop_luc_g5F	AAACTTGATCCTTTAAGCAGAAGCACAGGCTGCAGG
csm_gfp_stop_luc_g5R	TATCCCTGCAGCCTGTGCTTCTGCTTAAAGGATCAA
csm_gfp_stop_luc_g6F	AAACATCCTTTAAGCAGAAGCACAGGCTGCAGGGTG
csm_gfp_stop_luc_g6R	TATCCACCCTGCAGCCTGTGCTTCTGCTTAAAGGAT
Guides targeting fLuc-CFTR(W1282X) reporter and CFTR	
CFTR_1282_cr1F	AAACTGTGGTATCACTCCAAAGGCTTTCCTTCACTG
CFTR_1282_cr1R	TATCCAGTGAAGGAAAGCCTTTGGAGTGATACCACA
CFTR_1282_cr2F	AAACGGTATCACTCCAAAGGCTTTCCTTCACTGTTG
CFTR_1282_cr2R	TATCCAACAGTGAAGGAAAGCCTTTGGAGTGATACC
CFTR_1282_cr3F	AAACATCACTCCAAAGGCTTTCCTTCACTGTTGCAA
CFTR_1282_cr3R	TATCTTGCAACAGTGAAGGAAAGCCTTTGGAGTGAT
CFTR_1282_cr4F	AAACACTCCAAAGGCTTTCCTTCACTGTTGCAAAGT
CFTR_1282_cr4R	TATCACTTTGCAACAGTGAAGGAAAGCCTTTGGAGT
CFTR_1282_cr5F	AAACCCAAAGGCTTTCCTTCACTGTTGCAAAGTTAT
CFTR_1282_cr5R	TATCATAACTTTGCAACAGTGAAGGAAAGCCTTTGG
CFTR_1282_cr6F	AAACAAGGCTTTCCTTCACTGTTGCAAAGTTATTGA
CFTR_1282_cr6R	TATCTCAATAACTTTGCAACAGTGAAGGAAAGCCTT
CFTR_1282_cr7F	AAACGCTTTCCTTCACTGTTGCAAAGTTATTGAATC
CFTR_1282_cr7R	TATCGATTCAATAACTTTGCAACAGTGAAGGAAAGC
CFTR_1282_cr8F	AAACTTCCTTCACTGTTGCAAAGTTATTGAATCCCA
CFTR_1282_cr8R	TATCTGGGATTCAATAACTTTGCAACAGTGAAGGAA

Table S2.

Oligonucleotides used for generating plasmids encoding for crRNA or crRNA with Cas6-NLS gene

Name	Sequence 5`-3`
AN_Cas6F	GCCGGCCGGAGAATAAAAG
AN_PuroF	GCGATAGAGGGATCCCGC
AN_Afl II R	CTTAAGAAAAAGGCCGCGTTGC

Table S3.

Oligonucleotide primers used for Q5 SDM

Name	Sequence 5`-3`
SthCR_RFP_F	CGCGATGAAGCGATTCAGCGTCTCTGATATAAACCTAATTACCTCGAGAGGGGAC GCGGCCGCCACCATG
SthCR_RFP_R	TCTCGGTTTCCGTCCCCTCTCGAGGTAATTAGGTTTATATCGGATCTCTAGCGGAT CTGACGGTTCACTAAACCAGCTC
NLS-DisCas711_F	AAGCGGAAGGTCGGCGGTAGCACTACTATGAAGATTTCAATTGAATTC
NLS-DisCas711_R	CTTCTTTGGGGCCATGGTGGCGGCTCTCCCTATAGTG
Cas711_F1_F	AGAACTCAAACGCGGGGAATTCAAGAAAG
Cas711_F1_R	GATATCCCAGAGTTTATGGTCATCC
Cas711_F2_F	GGATGACCATAAACTCTGGGATATC
Cas711_F2_R	CTGGGAGAAATTTTTGCAGCACA
Cas711_F3_F	TGTGCTGCAAAAATTTCTCCCAG
Cas711_F3_R	CTTTCTTGAATTCCCCGCGTTTGAGTTCT

Table S4.

Oligonucleotides used for cloning Cas9 guides targeting RTCB gene

Name	Sequence 5`-3`
RTCB_sg1F	CACCGAATTGATGTTTGAGGAATTA
RTCB_sg1R	CAAATAATTCCTCAAACATCAATTC
RTCB_sg2F	CACCGGCAATGTGGCAGCCCTGCC
RTCB_sg2R	CAAAGGCAGGGCTGCCACATTGCC

Table S5.

Oligonucleotides used for cloning DisCas7-11 guide RNAs

Name	Sequence 5`-3`
discas711_gfp_stop_luc_g1F	GAACTTGATCCTTTAAGCAGAAGCACAGGCTGCAGG
discas711_gfp_stop_luc_g1R	AAAACCTGCAGCCTGTGCTTCTGCTTAAAGGATCAA
discas711_gfp_stop_luc_g2F	GAACTGATCCTTTAAGCAGAAGCACAGGCTGCAGGG
discas711_gfp_stop_luc_g2R	AAAACCCTGCAGCCTGTGCTTCTGCTTAAAGGATCA
discas711_gfp_stop_luc_g3F	GAACGATCCTTTAAGCAGAAGCACAGGCTGCAGGGT
discas711_gfp_stop_luc_g3R	AAAAACCCTGCAGCCTGTGCTTCTGCTTAAAGGATC
discas711_gfp_stop_luc_g4F	GAACATCCTTTAAGCAGAAGCACAGGCTGCAGGGTG
discas711_gfp_stop_luc_g4R	AAAACACCCTGCAGCCTGTGCTTCTGCTTAAAGGAT
discas711_gfp_stop_luc_g5F	GAACTCCTTTAAGCAGAAGCACAGGCTGCAGGGTGA
discas711_gfp_stop_luc_g5R	AAAATCACCCTGCAGCCTGTGCTTCTGCTTAAAGGA
discas711_gfp_stop_luc_g6F	GAACCCTTTAAGCAGAAGCACAGGCTGCAGGGTGAC
discas711_gfp_stop_luc_g6R	AAAAGTCACCCTGCAGCCTGTGCTTCTGCTTAAAGG
discas711_gfp_stop_luc_g7F	GAACCTTTAAGCAGAAGCACAGGCTGCAGGGTGACG
discas711_gfp_stop_luc_g7R	AAAACGTCACCCTGCAGCCTGTGCTTCTGCTTAAAG

Table S6.

Oligonucleotides used to amplify Cas9-targeted regions in the *RTCB* gene

Name	Sequence 5`-3`
RTCB_seq_F1	AGATGGAGCTTCAAATCCGTT
RTCB_seq_R1	TGTGGTTTTGAGGGTATGAGAAT
RTCB_seq_F2	GGTTATGTCTGGCTGTCCAAAG
RTCB_seq_R2	ATCTGGAATTTGAAGCTGGGTAG

Table S7.

Primers used for RT-qPCR and PCR

Name	Sequence 5`-3`
ACTB_F	AGAGCCTCGCCTTTGCC
ACTB_R	ATGCCGGAGCCGTTGTC
PPIB_cr1_qF1	GCGGCCGATGAGAAGAAGAA
PPIB_cr1_qR1	AGCTAAGGCCACAAAATTATCCAC
PPIB_cr2_qF1	CGCAGGCAAAGACACCAAC
PPIB_cr2_qR1	TTCCGCACCACCTCCA
PARK7_cr1_qF1	CCTACTCTGAGAATCGTGTGGA
PARK7_cr1_qR1	GAGCCGCCACCTCCTTG
PARK7_cr2_qF1	AGAGAAACAGGCCGTTAGGA
PARK7_cr2_qR1	GGCTGAGAAATCTCTGTGTAGTTG
gfp_stop_luc_qF1	GGATGGACCGTCACCCTG
gfp_stop_luc_qR1	TGTTTTTGGCGTCTTCCATACC
XIST_qF. Ref. 19	GTTGTATCGGGAGGCAGTAAGAATCATCTTT
XIST_qR Ref. 19	GAAAAGCACACAGCAAAGACAAAGAGGC
XIST_seq_F	GTCTTCTTGACACGTCCTCCA
XIST_seq_R	TCTGAACACGCCCTTAGCTT
CFTR_qF1	GGAAGAGTACTTTGTTATCAGCTTT
CFTR_qF2	CAGGGAAGAGTACTTTGTTATCAGC

Data S1. (separate file)

Analysis of the sequencing data in Figs. 1-4, fig. S1 and fig. S3-6; Sequences of plasmids created in this work.

References and Notes

1. M. Jinek, K. Chylinski, I. Fonfara, M. Hauer, J. A. Doudna, E. Charpentier, A programmable dual-RNA-guided DNA endonuclease in adaptive bacterial immunity. *Science* **337**, 816–821 (2012). doi:10.1126/science.1225829 Medline

2. G. Gasiunas, R. Barrangou, P. Horvath, V. Siksnys, Cas9–crRNA ribonucleoprotein complex mediates specific DNA cleavage for adaptive immunity in bacteria. *Proceedings of the National Academy of Sciences* **109**, (2012).

3. F. A. Ran, P. D. Hsu, J. Wright, V. Agarwala, D. A. Scott, F. Zhang, Genome engineering using the CRISPR-Cas9 system. *Nat. Protoc.* **8**, 2281–2308 (2013). doi:10.1038/nprot.2013.143 Medline

4. M. van Overbeek, D. Capurso, M. M. Carter, M. S. Thompson, E. Frias, C. Russ, J. S. Reece-Hoyes, C. Nye, S. Gradia, B. Vidal, J. Zheng, G. R. Hoffman, C. K. Fuller, A. P. May, DNA Repair Profiling Reveals Nonrandom Outcomes at Cas9-Mediated Breaks. *Mol. Cell* **63**, 633–646 (2016). doi:10.1016/j.molcel.2016.06.037 Medline

5. M. Kosicki, K. Tomberg, A. Bradley, Repair of double-strand breaks induced by CRISPR-Cas9 leads to large deletions and complex rearrangements. *Nat. Biotechnol.* **36**, 765–771 (2018). doi:10.1038/nbt.4192 Medline

6. Y. Fu, J. A. Foden, C. Khayter, M. L. Maeder, D. Reyon, J. K. Joung, J. D. Sander, High-frequency off-target mutagenesis induced by CRISPR-Cas nucleases in human cells. *Nat. Biotechnol.* **31**, 822–826 (2013). doi:10.1038/nbt.2623 Medline

7. P. D. Hsu, D. A. Scott, J. A. Weinstein, F. A. Ran, S. Konermann, V. Agarwala, Y. Li, E. J. Fine, X. Wu, O. Shalem, T. J. Cradick, L. A. Marraffini, G. Bao, F. Zhang, DNA targeting specificity of RNA-guided Cas9 nucleases. *Nat. Biotechnol.* **31**, 827–832 (2013). doi:10.1038/nbt.2647 Medline

8. V. Pattanayak, S. Lin, J. P. Guilinger, E. Ma, J. A. Doudna, D. R. Liu, High-throughput profiling of off-target DNA cleavage reveals RNA-programmed Cas9 nuclease specificity. *Nat. Biotechnol.* **31**, 839–843 (2013). doi:10.1038/nbt.2673 Medline

9. E. Haapaniemi, S. Botla, J. Persson, B. Schmierer, J. Taipale, CRISPR-Cas9 genome editing induces a p53-mediated DNA damage response. *Nat. Med.* **24**, 927–930 (2018). doi:10.1038/s41591-018-0049-z Medline

10. R. J. Ihry, K. A. Worringer, M. R. Salick, E. Frias, D. Ho, K. Theriault, S. Kommineni, J. Chen, M. Sondey, C. Ye, R. Randhawa, T. Kulkarni, Z. Yang, G. McAllister, C. Russ, J. Reece-Hoyes, W. Forrester, G. R. Hoffman, R. Dolmetsch, A. Kaykas, p53 inhibits CRISPR-Cas9 engineering in human pluripotent stem cells. *Nat. Med.* **24**, 939–946 (2018). doi:10.1038/s41591-018-0050-6 Medline

11. O. O. Abudayyeh, J. S. Gootenberg, S. Konermann, J. Joung, I. M. Slaymaker, D. B. T. Cox, S. Shmakov, K. S. Makarova, E. Semenova, L. Minakhin, K. Severinov, A. Regev, E. S. Lander, E. V. Koonin, F. Zhang, C2c2 is a single-component programmable RNA-guided RNA-targeting CRISPR effector. *Science* **353**, aaf5573 (2016). doi:10.1126/science.aaf5573 Medline

12. O. O. Abudayyeh, J. S. Gootenberg, P. Essletzbichler, S. Han, J. Joung, J. J. Belanto, V. Verdine, D. B. T. Cox, M. J. Kellner, A. Regev, E. S. Lander, D. F. Voytas, A. Y. Ting, F. Zhang, RNA targeting with CRISPR-Cas13. *Nature* **550**, 280–284 (2017). doi:10.1038/nature24049 Medline

13. S. Konermann, P. Lotfy, N. J. Brideau, J. Oki, M. N. Shokhirev, P. D. Hsu, Transcriptome Engineering with RNA-Targeting Type VI-D CRISPR Effectors. *Cell* **173**, 665–676.e14 (2018). doi:10.1016/j.cell.2018.02.033 Medline

14. J. Borrajo, K. Javanmardi, J. Griffin, S. J. St Martin, D. Yao, K. Hill, P. C. Blainey, B. Al-Shayeb, Programmable multi-kilobase RNA editing using CRISPR-mediated trans-splicing. bioRxiv 2023.08.18.553620. [Preprint] (2023); doi:10.1101/2023.08.18.553620.

15. D. B. T. Cox, J. S. Gootenberg, O. O. Abudayyeh, B. Franklin, M. J. Kellner, J. Joung, F. Zhang, RNA editing with CRISPR-Cas13. *Science* **358**, 1019–1027 (2017). doi:10.1126/science.aaq0180 Medline

16. O. O. Abudayyeh, J. S. Gootenberg, B. Franklin, J. Koob, M. J. Kellner, A. Ladha, J. Joung, P. Kirchgatterer, D. B. T. Cox, F. Zhang, A cytosine deaminase for programmable single-base RNA editing. *Science* **365**, 382–386 (2019). doi:10.1126/science.aax7063 Medline

17. C. R. Hale, P. Zhao, S. Olson, M. O. Duff, B. R. Graveley, L. Wells, R. M. Terns, M. P. Terns, RNA-guided RNA cleavage by a CRISPR RNA-Cas protein complex. *Cell* **139**, 945–956 (2009). doi:10.1016/j.cell.2009.07.040 Medline

18. G. Tamulaitis, M. Kazlauskiene, E. Manakova, Č. Venclovas, A. O. Nwokeoji, M. J. Dickman, P. Horvath, V. Siksnys, Programmable RNA shredding by the type III-A CRISPR-Cas system of Streptococcus thermophilus. *Mol. Cell* **56**, 506–517 (2014). doi:10.1016/j.molcel.2014.09.027 Medline

19. D. Colognori, M. Trinidad, J. A. Doudna, Precise transcript targeting by CRISPR-Csm complexes. *Nat. Biotechnol.* **41**, 1256–1264 (2023). doi:10.1038/s41587-022-01649-9 Medline

20. W. T. Woodside, N. Vantsev, R. J. Catchpole, S. C. Garrett, S. Olson, B. R. Graveley, M. P. Terns, Type III-A CRISPR systems as a versatile gene knockdown technology. *RNA* **28**, 1074–1088 (2022). doi:10.1261/rna.079206.122 Medline

21. T. Fricke, D. Smalakyte, M. Lapinski, A. Pateria, C. Weige, M. Pastor, A. Kolano, C. Winata, V. Siksnys, G. Tamulaitis, M. Bochtler, Targeted RNA Knockdown by a Type III CRISPR-Cas Complex in Zebrafish. *CRISPR J.* **3**, 299–313 (2020). doi:10.1089/crispr.2020.0032 Medline

22. NIH, ClinVar, https://www.ncbi.nlm.nih.gov/clinvar

23. L. V. Sharova, A. A. Sharov, T. Nedorezov, Y. Piao, N. Shaik, M. S. H. Ko, Database for mRNA half-life of 19 977 genes obtained by DNA microarray analysis of pluripotent and differentiating mouse embryonic stem cells. *DNA Res.* **16**, 45–58 (2009). doi:10.1093/dnares/dsn030 Medline

24. Y. Lu, F.-X. Liang, X. Wang, A synthetic biology approach identifies the mammalian UPR RNA ligase RtcB. *Mol. Cell* **55**, 758–770 (2014). doi:10.1016/j.molcel.2014.06.032 Medline

25. J. Jurkin, T. Henkel, A. F. Nielsen, M. Minnich, J. Popow, T. Kaufmann, K. Heindl, T. Hoffmann, M. Busslinger, J. Martinez, The mammalian tRNA ligase complex mediates splicing of XBP1 mRNA and controls antibody secretion in plasma cells. *EMBO J.* **33**, 2922–2936 (2014). doi:10.15252/embj.201490332 Medline

26. J. Popow, M. Englert, S. Weitzer, A. Schleiffer, B. Mierzwa, K. Mechtler, S. Trowitzsch, C. L. Will, R. Lührmann, D. Söll, J. Martinez, HSPC117 is the essential subunit of a human tRNA splicing ligase complex. *Science* **331**, 760–764 (2011). doi:10.1126/science.1197847 Medline

27. A. Kroupova, F. Ackle, I. Asanović, S. Weitzer, F. M. Boneberg, M. Faini, A. Leitner, A. Chui, R. Aebersold, J. Martinez, M. Jinek, Molecular architecture of the human tRNA ligase complex. *eLife* **10**, e71656 (2021). doi:10.7554/eLife.71656 Medline

28. L. E. Maquat, G. G. Carmichael, Quality control of mRNA function. *Cell* **104**, 173–176 (2001). doi:10.1016/S0092-8674(01)00202-1 Medline

29. A. Wutz, T. P. Rasmussen, R. Jaenisch, Chromosomal silencing and localization are mediated by different domains of Xist RNA. *Nat. Genet.* **30**, 167–174 (2002). doi:10.1038/ng820 Medline

30. J. Minks, S. E. L. Baldry, C. Yang, A. M. Cotton, C. J. Brown, XIST-induced silencing of flanking genes is achieved by additive action of repeat a monomers in human somatic cells. *Epigenetics Chromatin* **6**, 23 (2013). doi:10.1186/1756-8935-6-23 Medline

31. S. P. B. van Beljouw, A. C. Haagsma, A. Rodríguez-Molina, D. F. van den Berg, J. N. A. Vink, S. J. J. Brouns, The gRAMP CRISPR-Cas effector is an RNA endonuclease complexed with a caspase-like peptidase. *Science* **373**, 1349–1353 (2021). doi:10.1126/science.abk2718 Medline

32. A. Özcan, R. Krajeski, E. Ioannidi, B. Lee, A. Gardner, K. S. Makarova, E. V. Koonin, O. O. Abudayyeh, J. S. Gootenberg, Programmable RNA targeting with the single-protein CRISPR effector Cas7-11. *Nature* **597**, 720–725 (2021). doi:10.1038/s41586-021-03886-5 Medline

33. C. Schmitt-Ulms, A. Kayabolen, M. Manero-Carranza, N. Zhou, K. Donnelly, S. Pia Nuccio, K. Kato, H. Nishimasu, J. S. Gootenberg, O. O. Abudayyeh, Programmable RNA writing with trans-splicing. bioRxiv 2024.01.31.578223 [Preprint] (2024); doi:10.1101/2024.01.31.578223v1.

34. S. M. Rowe, K. Varga, A. Rab, Z. Bebok, K. Byram, Y. Li, E. J. Sorscher, J. P. Clancy, Restoration of W1282X CFTR activity by enhanced expression. *Am. J. Respir. Cell Mol. Biol.* **37**, 347–356 (2007). doi:10.1165/rcmb.2006-0176OC Medline

35. E. Nagy, L. E. Maquat, A rule for termination-codon position within intron-containing genes: When nonsense affects RNA abundance. *Trends Biochem. Sci.* **23**, 198–199 (1998). doi:10.1016/S0968-0004(98)01208-0 Medline

36. Y. J. Kim, T. Nomakuchi, F. Papaleonidopoulou, L. Yang, Q. Zhang, A. R. Krainer, Gene-specific nonsense-mediated mRNA decay targeting for cystic fibrosis therapy. *Nat. Commun.* **13**, 2978 (2022). doi:10.1038/s41467-022-30668-y Medline

37. A. Nemudryi, A. Nemudraia, J. E. Nichols, A. M. Scherffius, T. Zahl, B. Wiedenheft, CRISPR-based engineering of RNA viruses. *Sci. Adv.* **9**, eadj8277 (2023). doi:10.1126/sciadv.adj8277 Medline

38. K. Nemeth, R. Bayraktar, M. Ferracin, G. A. Calin, Non-coding RNAs in disease: From mechanisms to therapeutics. *Nat. Rev. Genet.* **25**, 211–232 (2024). doi:10.1038/s41576-023-00662-1 Medline

39. R. Batra, D. A. Nelles, E. Pirie, S. M. Blue, R. J. Marina, H. Wang, I. A. Chaim, J. D. Thomas, N. Zhang, V. Nguyen, S. Aigner, S. Markmiller, G. Xia, K. D. Corbett, M. S. Swanson, G. W. Yeo, Elimination of Toxic Microsatellite Repeat Expansion RNA by RNA-Targeting Cas9. *Cell* **170**, 899–912.e10 (2017). doi:10.1016/j.cell.2017.07.010 Medline

40. R. Vaz-Drago, N. Custódio, M. Carmo-Fonseca, Deep intronic mutations and human disease. *Hum. Genet.* **136**, 1093–1111 (2017). doi:10.1007/s00439-017-1809-4 Medline

41. P. Irmisch, I. Mogila, B. Samatanga, G. Tamulaitis, R. Seidel, Retention of the RNA ends provides the molecular memory for maintaining the activation of the Csm complex. *Nucleic Acids Res.* gkae080 (2024). doi:10.1093/nar/gkae080 Medline

42. Y. Ben-Ari, Y. Brody, N. Kinor, A. Mor, T. Tsukamoto, D. L. Spector, R. H. Singer, Y. Shav-Tal, The life of an mRNA in space and time. *J. Cell Sci.* **123**, 1761–1774 (2010). doi:10.1242/jcs.062638 Medline

43. K. N. D'Orazio, R. Green, Ribosome states signal RNA quality control. *Mol. Cell* **81**, 1372–1383 (2021). doi:10.1016/j.molcel.2021.02.022 Medline

44. G. Dugar, R. T. Leenay, S. K. Eisenbart, T. Bischler, B. U. Aul, C. L. Beisel, C. M. Sharma, CRISPR RNA-Dependent Binding and Cleavage of Endogenous RNAs by the *Campylobacter jejuni* Cas9. *Mol. Cell* **69**, 893–905.e7 (2018). doi:10.1016/j.molcel.2018.01.032 Medline

45. M. R. O'Connell, B. L. Oakes, S. H. Sternberg, A. East-Seletsky, M. Kaplan, J. A. Doudna, Programmable RNA recognition and cleavage by CRISPR/Cas9. *Nature* **516**, 263–266 (2014). doi:10.1038/nature13769 Medline

46. B. A. Rousseau, Z. Hou, M. J. Gramelspacher, Y. Zhang, Programmable RNA Cleavage and Recognition by a Natural CRISPR-Cas9 System from Neisseria meningitidis. *Mol. Cell* **69**, 906–914.e4 (2018). doi:10.1016/j.molcel.2018.01.025 Medline

47. S. C. Strutt, R. M. Torrez, E. Kaya, O. A. Negrete, J. A. Doudna, RNA-dependent RNA targeting by CRISPR-Cas9. *eLife* **7**, e32724 (2018). doi:10.7554/eLife.32724 Medline

48. J. P. K. Bravo, T. Hallmark, B. Naegle, C. L. Beisel, R. N. Jackson, D. W. Taylor, RNA targeting unleashes indiscriminate nuclease activity of CRISPR-Cas12a2. *Nature* **613**, 582–587 (2023). doi:10.1038/s41586-022-05560-w Medline

49. O. Dmytrenko, G. C. Neumann, T. Hallmark, D. J. Keiser, V. M. Crowley, E. Vialetto, I. Mougiakos, K. G. Wandera, H. Domgaard, J. Weber, T. Gaudin, J. Metcalf, B. N. Gray, M. B. Begemann, R. N. Jackson, C. L. Beisel, Cas12a2 elicits abortive infection through RNA-triggered destruction of dsDNA. *Nature* **613**, 588–594 (2023). doi:10.1038/s41586-022-05559-3 Medline

50. W. X. Yan, P. Hunnewell, L. E. Alfonse, J. M. Carte, E. Keston-Smith, S. Sothiselvam, A. J. Garrity, S. Chong, K. S. Makarova, E. V. Koonin, D. R. Cheng, D. A. Scott, Functionally diverse type V CRISPR-Cas systems. *Science* **363**, 88–91 (2019). doi:10.1126/science.aav7271 Medline

51. M. Jinek, F. Jiang, D. W. Taylor, S. H. Sternberg, E. Kaya, E. Ma, C. Anders, M. Hauer, K. Zhou, S. Lin, M. Kaplan, A. T. Iavarone, E. Charpentier, E. Nogales, J. A. Doudna, Structures of Cas9 endonucleases reveal RNA-mediated conformational activation. *Science* **343**, 1247997 (2014). doi:10.1126/science.1247997 Medline

52. T. Yamano, H. Nishimasu, B. Zetsche, H. Hirano, I. M. Slaymaker, Y. Li, I. Fedorova, T. Nakane, K. S. Makarova, E. V. Koonin, R. Ishitani, F. Zhang, O. Nureki, Crystal Structure of Cpf1 in Complex with Guide RNA and Target DNA. *Cell* **165**, 949–962 (2016). doi:10.1016/j.cell.2016.04.003 Medline

53. Y. Yuan, F. M. Stumpf, L. A. Schlor, O. P. Schmidt, P. Saumer, L. B. Huber, M. Frese, E. Höllmüller, M. Scheffner, F. Stengel, K. Diederichs, A. Marx, Chemoproteomic discovery of a human RNA ligase. *Nat. Commun.* **14**, 842 (2023). doi:10.1038/s41467-023-36451-x Medline

54. H.-H. Wessels, A. Méndez-Mancilla, X. Guo, M. Legut, Z. Daniloski, N. E. Sanjana, Massively parallel Cas13 screens reveal principles for guide RNA design. *Nat. Biotechnol.* **38**, 722–727 (2020). doi:10.1038/s41587-020-0456-9 Medline

55. H.-H. Wessels, A. Stirn, A. Méndez-Mancilla, E. J. Kim, S. K. Hart, D. A. Knowles, N. E. Sanjana, Prediction of on-target and off-target activity of CRISPR–Cas13d guide RNAs using deep learning. *Nat. Biotechnol.* **42**, 628–637 (2023) doi:10.1038/s41587-023-01830-8 Medline

56. L. Cong, F. A. Ran, D. Cox, S. Lin, R. Barretto, N. Habib, P. D. Hsu, X. Wu, W. Jiang, L. A. Marraffini, F. Zhang, Multiplex genome engineering using CRISPR/Cas systems. *Science* **339**, 819–823 (2013). doi:10.1126/science.1231143 Medline

57. L. Villiger, J. Joung, L. Koblan, J. Weissman, O. O. Abudayyeh, J. S. Gootenberg, CRISPR technologies for genome, epigenome and transcriptome editing. *Nat. Rev. Mol. Cell Biol.* (2024). doi:10.1038/s41580-023-00697-6 Medline

58. A. Nemudraia, A. Nemudryi, B. Wiedenheft, Amplicon sequencing of human mRNA and reporter mRNA targeted with type III-A CRISPR complex of Streptococcus thermophilus, NCBI (2024); https://www.ncbi.nlm.nih.gov/bioproject/PRJNA1099688/

59. A. Nemudraia, A. Nemudryi, B. Wiedenheft, Code for generating figures and analyzing amplicon sequencing of human mRNA and reporter mRNA targeted with type III-A CRISPR complex from Streptococcus thermophiles, Zenodo (2024); doi: 10.5281/zenodo.10966960

60. M. W. Shen, M. Arbab, J. Y. Hsu, D. Worstell, S. J. Culbertson, O. Krabbe, C. A. Cassa, D. R. Liu, D. K. Gifford, R. I. Sherwood, Predictable and precise template-free CRISPR editing of pathogenic variants. *Nature* **563**, 646–651 (2018). doi:10.1038/s41586-018-0686-x Medline

61. K. Kato, W. Zhou, S. Okazaki, Y. Isayama, T. Nishizawa, J. S. Gootenberg, O. O. Abudayyeh, H. Nishimasu, Structure and engineering of the type III-E CRISPR-Cas7-11

effector complex. *Cell* **185**, 2324–2337.e16 (2022). doi:10.1016/j.cell.2022.05.003 Medline

62. D. Conant, T. Hsiau, N. Rossi, J. Oki, T. Maures, K. Waite, J. Yang, S. Joshi, R. Kelso, K. Holden, B. L. Enzmann, R. Stoner, Inference of CRISPR Edits from Sanger Trace Data. *CRISPR J.* **5**, 123–130 (2022). doi:10.1089/crispr.2021.0113 Medline

63. D. Kim, J.-Y. Lee, J.-S. Yang, J. W. Kim, V. N. Kim, H. Chang, The Architecture of SARS-CoV-2 Transcriptome. *Cell* **181**, 914–921.e10 (2020). doi:10.1016/j.cell.2020.04.011 Medline

64. Y.-C. Lin, M. Boone, L. Meuris, I. Lemmens, N. Van Roy, A. Soete, J. Reumers, M. Moisse, S. Plaisance, R. Drmanac, J. Chen, F. Speleman, D. Lambrechts, Y. Van de Peer, J. Tavernier, N. Callewaert, Genome dynamics of the human embryonic kidney 293 lineage in response to cell biology manipulations. *Nat. Commun.* **5**, 4767 (2014). doi:10.1038/ncomms5767 Medline